Simulation study of a two-dimensional system of semiflexible polymers

Marjolein Dijkstra and Daan Frenkel
Fundamenteel Onderzoek der Materie—Instituut voor Atoom- en Molecuulfysica, Kruislaan 407, 1098 SJ Amsterdam, The Netherlands
(Received 28 February 1994)

We report computer simulations of a two-dimensional system of semiflexible polymers consisting of infinitesimally thin hard segments connected by joints of variable flexibility. As the density is increased, we observe a transition from the isotropic phase to a "nematic" phase with quasi-long-range orientational order. This transition appears to be of the Kosterlitz-Thouless type. We observe that, whereas at low densities the most rigid polymers have the lowest compressibility, the opposite is true at high densities. We argue that such behavior is to be expected. Finally, we study the scaling behavior of the elastic constants for splay and bend in the nematic phase and find good agreement with the relevant theoretical predictions.

PACS number(s): 64.70.Md, 61.25.Hq, 61.20.Ja

I. INTRODUCTION

The study of semiflexible polymers was initiated by Flory in 1956 [1]. Still, the statistical behavior of bulk systems of semiflexible polymers is incompletely understood. Flory modeled the polymers by self-avoiding random walks on a three-dimensional lattice and defined the equilibrium flexibility as the fraction of bonds that are bent. In his mean-field calculation, he obtained a first-order phase transition from an isotropic phase to an orientationally ordered state, when the flexibility exceeds a critical value. Other mean-field theories [2–4] also predict this phase transition for three-dimensional lattice polymers. However, these results have been disputed on the basis of several exactly solvable models for three-dimensional polymers which show a continuous phase transition [5,6]. It would seem that computer simulations could be used to investigate the phase behavior of semiflexible polymers. However, somewhat surprisingly, long-range orientational order has thus far not been observed in computer simulations of two- and three-dimensional athermal lattice polymers [7–10]. In particular, in the simulations of Baumgärtner [7] (athermal polymers on a square and cubic lattice), Kolinsky *et al.* [8] (tetrahedral lattice), and Rodriguez *et al.* [9] (bond fluctuation model in two dimensions) only a transition to ordered domains is observed. The linear dimension of these domains is of the order of the contour length of the polymer. Only upon inclusion in the model of an attractive interaction between two nearest neighbor segments oriented parallel is an isotropic-nematic phase transition observed [7,8]. The reason why the athermal semiflexible polymers do not seem to form an orientationally ordered phase may, at least in part, be due to the fact that the simulations referred to above were all performed on lattice models. It is therefore interesting to consider an off-lattice system of continuously deformable polymers. Theories for the phase behavior of off-lattice semiflexible polymers all do predict an isotropic to nematic phase transition [11,12] in three dimensions. Recently, a continuous isotropic-nematic phase transition was predicted [13] for a two-dimensional system of semiflexible polymers.

In this paper, we present a simulation study of a two-dimensional off-lattice model of semiflexible polymers. In particular, we investigate whether this system exhibits an isotropic to nematic phase transition. We performed a series of grand canonical Monte Carlo (GCMC) simulations [14] of semiflexible polymers with varying flexibility. For infinitely stiff polymers, i.e., needles, simulations have been performed earlier by Frenkel and Eppenga [15]. In these simulations, an isotropic to "nematic" phase transition of the Kosterlitz-Thouless type was observed.

We found that, for the simulations reported in this paper, the conventional Monte Carlo schemes (Metropolis sampling and reptation) were not sufficiently efficient to ensure rapid equilibration. For a faster equilibration of the polymers we used the configurational bias Monte Carlo (CBMC) method [16,17]. This method will be discussed in Sec. II. For more technical details on the implementation of the CBMC method in the GCMC simulation, we refer to the Appendix. In Sec. III we present the results and discussion.

II. MODEL AND COMPUTATIONAL TECHNIQUE

We performed GCMC simulations of a two-dimensional system of semiflexible polymers. The chains consist of ten infinitesimally thin hard segments connected to each other. The bending energy for a joint between two segments, i and $i-1$, is

$$u^{id}_{\hat{\mathbf{w}}_{i-1}\hat{\mathbf{w}}_i} = \frac{1}{2} C \, (\theta_{\hat{\mathbf{w}}_{i-1}\hat{\mathbf{w}}_i})^2 \, , \tag{1}$$

where $\theta_{\hat{\mathbf{w}}_{i-1}\hat{\mathbf{w}}_i}$ is the angle between the unit vectors $\hat{\mathbf{w}}_{i-1}$ and $\hat{\mathbf{w}}_i$ that specify, respectively, the orientations of the segments $i-1$ and i. The bending elastic modulus C is the bending energy per unit length. The segment length was chosen as our unit of length. The persistence length l_p is related to the bending elastic modulus C:

$$l_p = \frac{C}{k_B T} . \quad (2)$$

In a GCMC simulation, the chemical potential, the temperature, and the "volume" of the system are fixed quantities. The side of the periodic box used in our simulations was 30 segment lengths. In our Monte Carlo simulations we had to ensure that no trial move would result in a hard-core overlap of the polymer segments. To test whether a trial move generated such an overlap, we used the criterion described in Ref. [15]. The following trial moves were performed.

(1) Reptation: Remove a segment from one end of the polymer. Generate one trial segment at either end of the polymer in such a way that the probability of finding a given angle with the previous segment is given by the Boltzmann weight associated with the bond bending. Accept this segment if it has no overlap with another segment. If the move is not accepted, reset the segment to its original position.

(2) Regrow a whole polymer at a random position and with a random orientation using the CBMC method [16]. Below, the procedure is only briefly sketched. For more technical details we refer to the Appendix. The construction of a chain proceeds segment by segment. To add a segment, we generate a fixed number of trial segments according to the internal (bond-bending) Boltzmann factors. The Boltzmann factors, associated with the nonbonded interaction, are either zero (if the segment overlaps with another) or one (if there is no overlap). We refer to the Boltzmann factors associated with nonbonded interaction as "external" to distinguish them from the "internal" Boltzmann factors associated with bond bending. We select the new segment with a probability that is proportional to the external Boltzmann factor. The new polymer conformation will now be accepted with a certain probability that can be derived from the condition of detailed balance (see Ref. [16]).

(3) Remove or insert a polymer in the system. For the insertion of the polymer we used the same procedure as above. This trial move, insertion or removal, will be accepted with a probability that satisfies the condition of detailed balance and is described in more detail in the Appendix.

In our simulations we calculated the average density ρ, the pressure P, and the elastic constants for the splay and the bend, respectively, K_1 and K_3, as a function of the imposed chemical potential μ and of the chosen persistence length l_P. The pressure is calculated by virtual volume changes. In this method, we use the fact that the pressure can be obtained by differentiation of the thermodynamic potential with respect to the volume. To this end we must compute the acceptance ratio [18] of virtual trial moves that decrease and increase the volume of the system. For hard convex bodies, the acceptance of virtual expansions is always one and the method reduces to that described in Ref. [19]. However, in the present case for polymers there is a small but finite probability to reject virtual expansions. For the sake of comparison, we also computed the pressure by integrating the Gibbs-Duhem equation. This equation shows the relationship between a change in the temperature and pressure to a change in the chemical potential:

$$d\mu = -\frac{S}{N} dT + \frac{V}{N} dP . \quad (3)$$

We can now compute the pressure by integrating the Gibbs-Duhem equation at constant temperature:

$$dP = \rho \, d\mu . \quad (4)$$

In the nematic phase the orientational distribution function is symmetric around a preferred direction $\hat{\mathbf{n}}$, i.e., the nematic director. A deformation of the uniform alignment of the director in a nematic results in an elastic restoring force. The constants of proportionality between the deformation and the restoring forces are the Frank elastic constants. The deformation free energy F_D density for a two-dimensional nematic has the following form:

$$F_D = \frac{1}{2} K_1 [\nabla \cdot \hat{\mathbf{n}}(\mathbf{r})]^2 + \frac{1}{2} K_3 [\nabla \times \hat{\mathbf{n}}(\mathbf{r})]^2 . \quad (5)$$

In Fourier language this is equivalent to

$$F_D = \frac{1}{2V} \sum_{\mathbf{q}} K_1 [\mathbf{q} \cdot \hat{\mathbf{n}}(\mathbf{q})]^2 + \frac{1}{2} K_3 [\mathbf{q} \times \hat{\mathbf{n}}(\mathbf{q})]^2 , \quad (6)$$

where V is the volume of the system. If we decompose $\mathbf{q}$ in components $q_\perp$ and $q_\parallel$, respectively, perpendicular and parallel to the nematic director $\hat{\mathbf{n}}$ we arrive at

$$F_D = \frac{1}{2V} \sum_{\mathbf{q}} |n_\perp(\mathbf{q})|^2 (K_1 q_\perp^2 + K_3 q_\parallel^2) \quad (7)$$

and the equipartition theorem yields

$$\langle |n_\perp|^2 \rangle = \frac{V k_B T}{K_1 q_\perp^2 + K_3 q_\parallel^2} . \quad (8)$$

The nematic director in a system of N polymers consisting of L segments can be calculated by finding the eigenvalues and eigenvectors of the tensor order parameter density Q.

$$Q_{\alpha\beta}(r) = \frac{1}{L} \sum_{k=1}^{N} \sum_{j=1}^{L} [2 \hat{\mathbf{w}}_\alpha^{k,j} \hat{\mathbf{w}}_\beta^{k,j} - \delta_{\alpha\beta}] \delta(\mathbf{r} - \mathbf{r}_{k,j}) , \quad (9)$$

where $\hat{\mathbf{w}}_\alpha^{k,j}$ is the αth Cartesian coordinate of the unit vectors specifying the orientation of segment j of polymer k and $\mathbf{r}_{k,j}$ the position of this segment. The nematic director is the eigenvector that corresponds with the largest eigenvalue. The ensemble averaged value of Q (i.e., averaged over all segments in the system) after diagonalizing of the tensor is

$$\langle Q \rangle = \rho S (2 \hat{\mathbf{n}} \hat{\mathbf{n}} - \mathbf{I}), \quad (10)$$

where S is the largest eigenvalue of the tensor order parameter Q and ρ is equal to the number density of polymers. As $\hat{\mathbf{n}}$ is a unit vector, a small fluctuation in the orientation of the director will, to first order, be perpen-

dicular to the nematic director. A small fluctuation in the nematic director can now be expressed in Q.

$$Q_{\hat{\mathbf{n}}_\perp \hat{\mathbf{n}}_\parallel}(\mathbf{q}) = 2\hat{\mathbf{n}}_\parallel \delta\hat{\mathbf{n}}_\perp S\rho \tag{11}$$

and

$$\langle |Q_{\hat{\mathbf{n}}_\perp \hat{\mathbf{n}}_\parallel}(\mathbf{q})|^2 \rangle = \left| \frac{1}{L} \sum_{k=1}^{N} \sum_{j=1}^{L} [2\hat{\mathbf{w}}^{k,j}_{\hat{\mathbf{n}}_\perp} \hat{\mathbf{w}}^{k,j}_{\hat{\mathbf{n}}_\parallel}] \exp(i\mathbf{q} \cdot \mathbf{r}_{k,j}) \right|^2 \tag{12}$$

$$= \frac{4S^2\rho^2 V k_B T}{K_1 q_\perp^2 + K_3 q_\parallel^2} . \tag{13}$$

Thus if we calculate $\langle |Q_{\hat{\mathbf{n}}_\perp \hat{\mathbf{n}}_\parallel}|^2 \rangle$ for $\mathbf{q}$ parallel and perpendicular to the nematic director, we can compute the elastic constants K_1 and K_3. The analogous expression for three-dimensional (3D) nematics was used in Refs. [20,21].

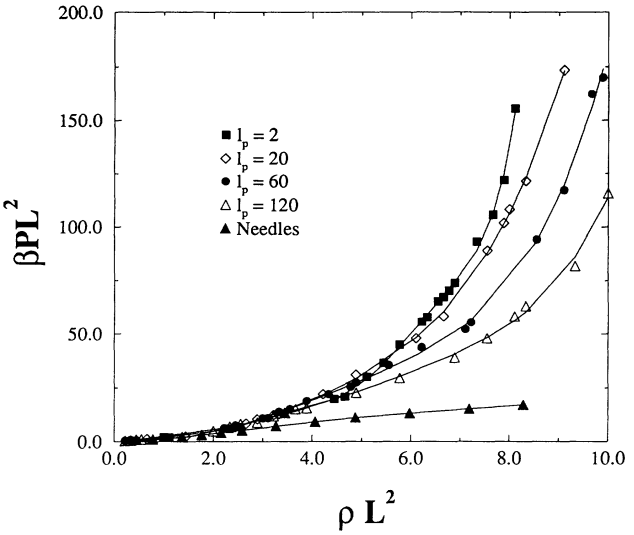

FIG. 1. Pressure versus the density for different values for the flexibility of the two-dimensional semiflexible polymers with L the length of the polymer.

III. RESULTS AND DISCUSSION

We performed GCMC simulations of semiflexible polymers with different persistence length (l_P = 2, 20, 60, and 120) in order to investigate the influence of flexibility on the equation of state. In a GCMC simulation the chemical potential, the volume, and the temperature are fixed quantities. The chemical potential was chosen such that the dimensionless or reduced density ρL^2 varied from 0.2 to 10. The initial configuration from which the first runs were started was one in which all the polymers were directed in the same direction but randomly positioned in the periodic box. Subsequent runs were started from previously equilibrated configurations at a higher or lower chemical potential. Most runs consisted of $1 \times 10^5 - 1 \times 10^7$ trial moves per particle. Most trial moves were simple reptation moves. On average once every three reptation moves, a polymer is completely regrown at a random position in the periodic box using the CBMC method. Once every ten reptation moves, a trial move to insert or to remove a particle was attempted. In order to investigate the pressure dependence at low densities and the elastic constants in the nematic phase, canonical ensemble simulations (number of particles, volume, and temperature are fixed) were performed for systems with densities ranging from 0.2 to 1 and from 10 to 70 in reduced units. Figure 1 shows a plot of the pressure versus the reduced density for different values of the persistence length of the polymers. For the sake of comparison the results for hard needles (Ref. [15]) have also been plotted in Fig. 1. Earlier simulations by Dickman [10] indicated that for a dilute system the pressure increases dramatically with increasing stiffness, but it is nearly independent of stiffness in dense systems [10]. However, for high densities we observe an increase in the pressure when the polymers become more flexible. This effect is to be expected because for dense systems the confinement free energy plays a role. An increase in the flexibility of the polymers results in a larger confinement free energy and the pressure will increase rapidly with larger flexibility [17].

At low densities, the pressure can be approximated by the virial expansion.

$$\frac{P}{k_B T} = \rho + B_2 \rho^2 + \cdots . \tag{14}$$

For hard-core systems, the second virial coefficient B_2 is a measure of the pair excluded volume of the polymers. For flexible chains the excluded volume is smaller than for stiff chains and therefore we expect that the pressure is smaller for more flexible chains. At low densities ($\rho L^2 < 1$) we do indeed observe an increase in pressure with stiffness (see Fig. 2) and our results agree qualitatively with those of Ref. [10] at low densities.

For the sake of comparison, we computed the virial coefficient B_2 numerically and plotted the virial expansion [Eq. (14)] truncated at the second virial coefficient in Fig. 2. For semiflexible polymers with persistence length 2 and 120, we found, respectively, $B_2 = 0.2393 \pm 0.0003$ and 0.3166 ± 0.0002 in units of L^2. The latter value approaches the value for the second virial coefficient for hard needles, i.e., $1/\pi$ in units of L^2. As can be seen in Fig. 2, the pressure computed in our MC simulations reduces to the value predicted on the basis of the second-virial coefficient, in the low-density limit.

In order to test our calculations of the pressure by virtual volume changes, we also computed the pressure by integrating the Gibbs-Duhem equation. Figure 3 shows that the pressure calculations by virtual volume changes agree well with the pressure obtained by integration of the Gibbs-Duhem equation.

The orientational distribution function $g_2(r) = \langle \cos\{2[\theta(0) - \theta(r)]\} \rangle$ is plotted in Fig. 4 as a function of r (in units of the segment length) for a system with a density of about 8 in reduced units. For large flexibility ($l_P = 2$), the orientational order dies out over a distance

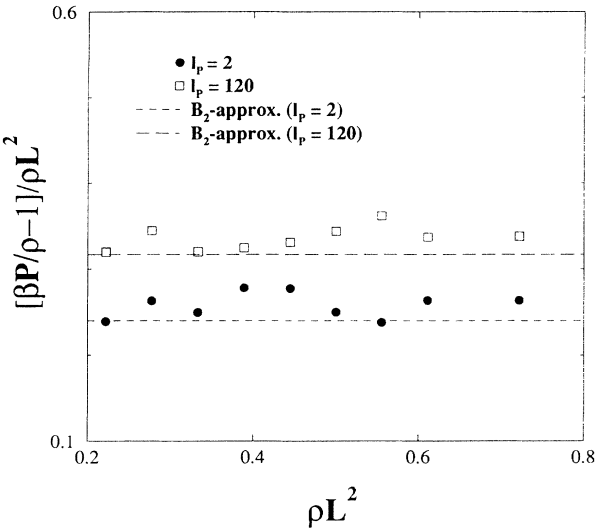

FIG. 2. Pressure versus the density for semiflexible polymers of persistence length 2 (black circles) and 120 (open squares) in the low-density regime. The dashed line and the long-dashed line correspond with the B_2 approximation for semiflexible polymers of, respectively, persistence length 2 and 120. L denotes the length of the polymer.

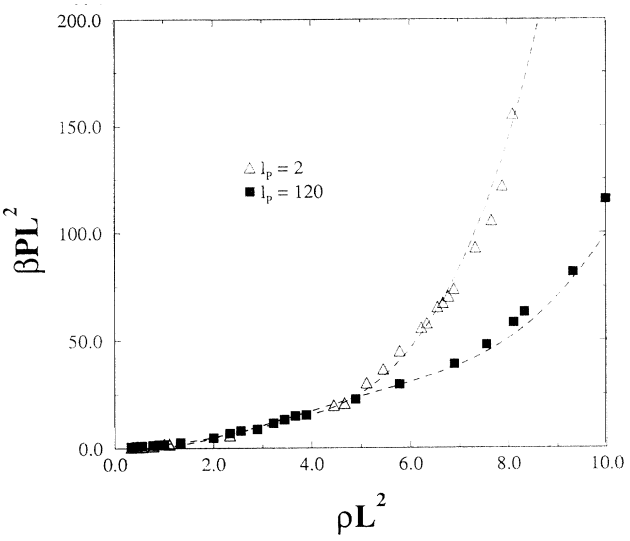

FIG. 3. The pressure calculated by integration of the Gibbs-Duhem equation for persistence length $l_P = 2$ and 120 (dashed line) and the pressure calculated by virtual volume changes (open triangles and black squares). L denotes the length of the polymer.

smaller than the length of the polymer. For stiffer chains, we find that the orientational order appears to decay algebraically. This algebraic decay of orientational order was also observed in a two-dimensional fluid of hard needles, which shows an isotropic-nematic phase transition of the Kosterlitz-Thouless type. For 2D nematics the Kosterlitz-Thouless transition occurs at a universal value of the renormalized elastic constant, i.e., $K = (K_3 K_1)^{1/2}$ [22]:

$$\frac{\pi K}{8 k_B T} = 1 \, . \tag{15}$$

We computed the elastic constants for the splay and the bend, respectively, K_1 and K_3. In Figs. 5 and 6, the elastic constants for, respectively, the bend and the splay are plotted versus the density. We observe that at high density the elastic constants increase with stiffness. This effect is to be expected, as a system consisting of more flexible chains is easier to deform. We also find that the elastic constants for the splay are smaller than for the bend. Using Eq. (15), we can now estimate the density at which a Kosterlitz-Thouless transition should occur. To this end, we fitted our data for the elastic constants as a function of the density for different per-

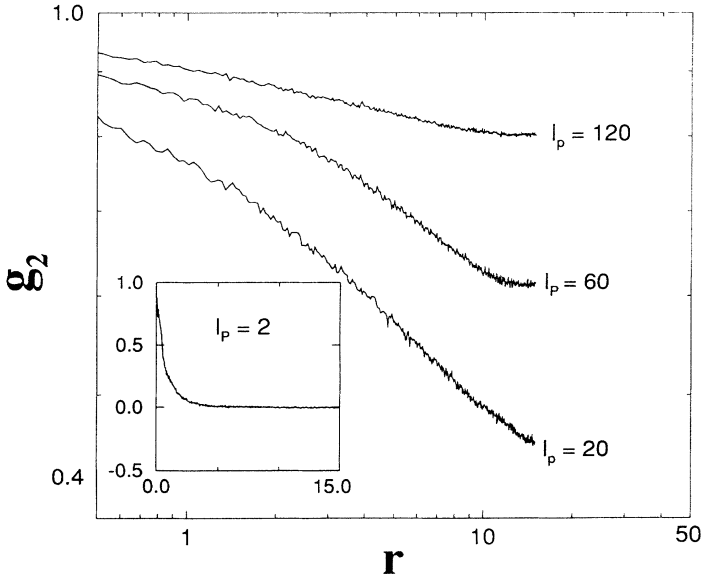

FIG. 4. The orientational distribution function $g_2(r) = \langle \cos\{2[\theta(0) - \theta(r)]\} \rangle$ versus r (in units of the segment length) for different values for the flexibility of the two-dimensional semiflexible polymers at a density of about 8 in reduced units.

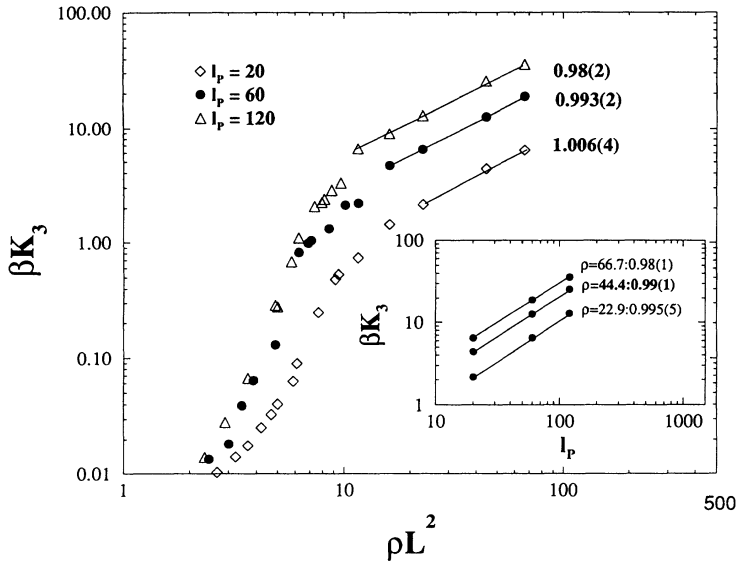

FIG. 5. The elastic constant for the bend as a function of the density. L denotes the length of the polymer. In order to investigate the scaling behavior, we have fitted the data for high density. The values for the slopes are plotted with the error in the last digit in parentheses.

sistence lengths. Using this fit, we computed the density at which K becomes larger than $8k_BT/\pi$. The densities ρ_{K-T} at which this happens are estimated to be $21.7 \pm 0.8, 16.1 \pm 0.5, 11.7 \pm 0.5$ in reduced units for, respectively, persistence length $l_P = 20, 60$, and 120 (see Fig. 7). For the sake of comparison, we have also plotted the value for hard needles (Ref. [15]) in Fig. 7.

In Fig. 8, we have shown typical configurations of the two-dimensional semiflexible polymer fluid with persistence length $l_P = 120$ at reduced densities $\rho L^2 = 4.89$, 9.11, and 22.22 and with persistence length $l_P = 20$ at reduced densities $\rho L^2 = 4.44$, 8.88, and 22.22. The snapshots for the highest density are well inside the nematic regime. The configurations at lower densities are isotropic, in spite of the fact that, due to finite size effects, the configurations look nematic. In Fig. 9, we have shown typical snapshots of the semiflexible polymer fluid with persistence length $l_P = 2$ at reduced densities $\rho L^2 = 5.11$ and 8.44. Both configurations are in the isotropic regime.

In the nematic phase, each polymer is strongly hindered by neighboring polymers and we can assume that each polymer is effectively confined to a tube with diameter D. The tube diameter D scales with the density as ρ^{-1}. The ratio of the elastic constants for the bend and for the splay is then expected to scale as follows [23]:

$$\frac{K_3}{K_1} \sim \left(\frac{\lambda}{D}\right)^2 . \tag{16}$$

A new length scale is introduced here, namely, the deflection length λ. The deflection length is the characteristic length scale for a semiflexible chain confined in a tube with diameter D. This length scale corresponds to the average distance between two successive deflection points of the chain in the tube and is found to scale as $l_P^{1/3}D^{2/3}$ [24,25]. It is not surprising that the ratio of the elastic constants follows Eq. (16), as the deflection length and the diameter are the characteristic length scales parallel and perpendicular to the nematic director. The bending

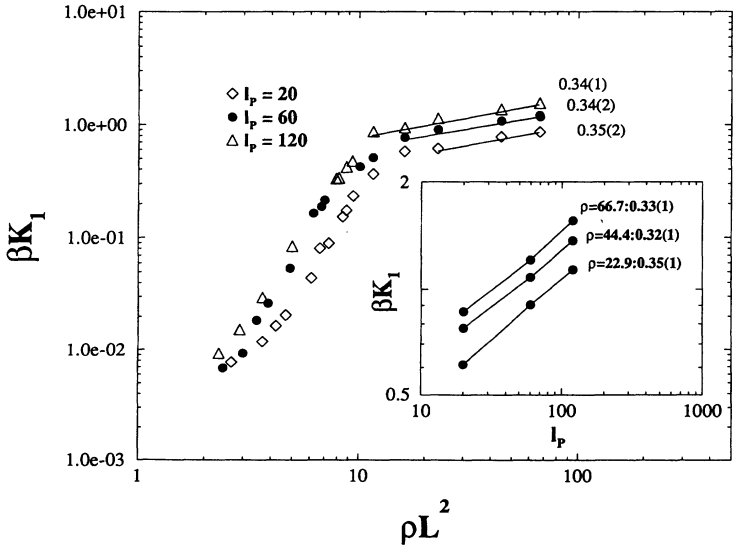

FIG. 6. The elastic constant for the splay as a function of the density. L denotes the length of the polymer. In order to investigate the scaling behavior, we have fitted the data for high density. The values for the slopes are plotted with the error in the last digit in parentheses.

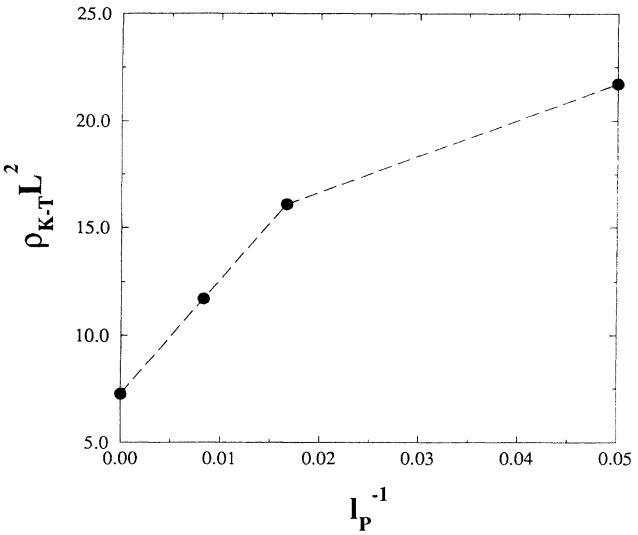

FIG. 7. The density at which the Kosterlitz-Thouless transition occurs versus the inverse persistence length flexibility for a two-dimensional system of semiflexible polymers with L the length of the polymers.

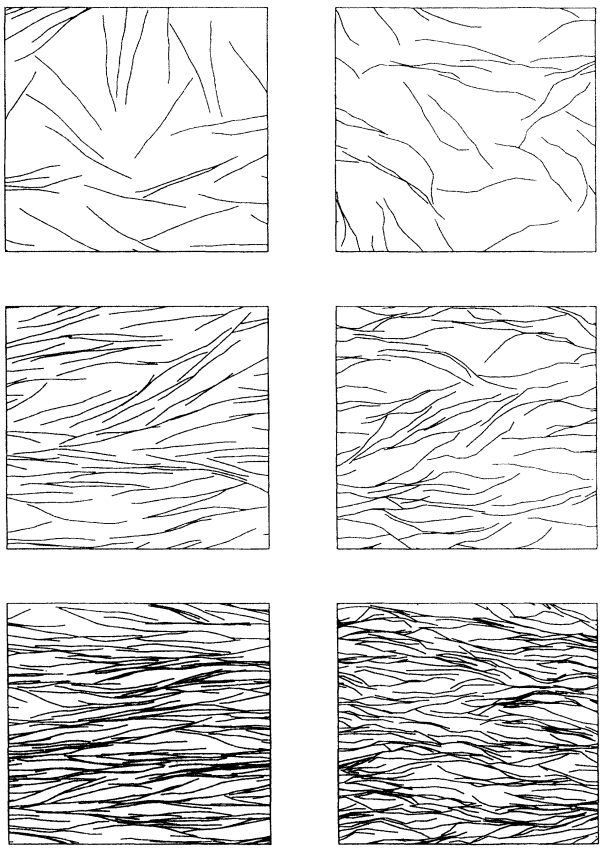

FIG. 8. Snapshots of the two-dimensional semiflexible polymers with persistence length $l_P = 120$ (left, density equal to 4.89, 9.11, and 22.22 in reduced units from top to bottom) and $l_P = 20$ (right, density equal to 4.44, 8.88, and 22.22 in reduced units from top to bottom). The size of the snapshots is 25 × 25 in units of the segment length.

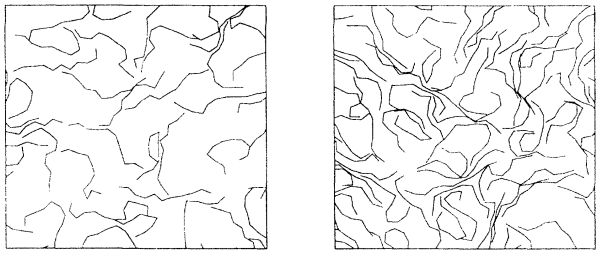

FIG. 9. Snapshots of the two-dimensional semiflexible polymers with persistence length $l_P = 2$ (density equal to 5.11 and 8.44 in reduced units from left to right). The size of the snapshots is 25 × 25 in units of the segment length.

elastic constant is directly related to the internal bending constant and the density and scales as [23]

$$K_3 \sim C\rho = \rho k_B T l_P \ . \tag{17}$$

Using Eqs. (16) and (17) we can derive the scaling behavior of the elastic constant for the splay with the density and the persistence length (i.e., $\sim \rho^{1/3} l_P^{1/3}$). It is, therefore, interesting to investigate the scaling behavior of the elastic constants at high densities. We find that both the bending elastic constant and the splay elastic constant scale as a power of the density ($K_1 \sim \rho^{\mu_1}$ and $K_3 \sim \rho^{\mu_3}$). We computed μ_1 and μ_3 for the different persistence lengths as shown in Figs. 5 and 6. We find $\mu_3 = 1.006 \pm 0.004, 0.993 \pm 0.002$, and 0.98 ± 0.02 for, respectively, persistence lengths $l_P = 20$, 60, and 120. Thus we do indeed find that the bending elastic constant scales linearly with the density for densities well inside the nematic regime. In Fig. 6, μ_1 is $0.35 \pm 0.02, 0.34 \pm 0.02$, and 0.34 ± 0.01 for, respectively, persistence lengths $l_P = 20$, 60, and 120. This value should be compared with 1/3 as expected on the basis of the scaling argument. Secondly, the bending elastic constant is found to scale as $\sim l_P^{\nu_3}$ and the splay elastic constant scales as $\sim l_P^{\nu_1}$. We computed ν_1 and ν_3 for the different densities as shown in the insets of Figs. 5 and 6. We find, respectively, $\nu_3 = 0.995 \pm 0.005, 0.99 \pm 0.01$, and 0.98 ± 0.01 for densities $\rho = 22.9$, 44.4, and 66.7 in reduced units. For ν_1 we find, respectively, $\nu_1 = 0.35 \pm 0.01, 0.32 \pm 0.01$, and 0.33 ± 0.01 for densities $\rho = 22.9$, 44.4, and 66.7 in reduced units. This should be compared with the values $\nu_3 = 1$ and $\nu_1 = 1/3$ predicted by theory. Thus our data are consistent with the scaling relations predicted theoretically.

In summary, we have performed simulations of a two-dimensional system of semiflexible polymers. For a dilute system the pressure decreases when the polymers become more flexible, but increases in dense systems. If we increase the density, we observe an isotropic-nematic phase transition with algebraic decay of orientational order. This transition appears to be of the Kosterlitz-Thouless type. The scaling behavior of the elastic constants is found to be in good agreement with the theoretical predictions.

ACKNOWLEDGMENTS

The work of the FOM Institute is part of the scientific program of FOM and is supported by the Nederlandse Organisatie voor Wetenschappelijk Onderzoek (NWO). We thank P. Bladon and Maria J. Ruiz Montero for a critical reading of the manuscript.

APPENDIX

One of the trial moves in a GCMC simulation is the exchange of particles with an infinitely large reservoir, which contains an ideal gas of the same particles (in the present case the ideal gas particles have internal bending energy). Direct insertion of all but the shortest flexible particles in a dense fluid has a prohibitively low probability, as it almost always results in an overlap with one of the other chains. We therefore employed an extension of the configurational bias Monte Carlo method [16] to GCMC simulations. In this algorithm, we bias the insertion of chains in such a way that the "holes" of the system are found. Below, we describe the algorithm.

Consider a trial move to insert a molecule in the system. We first choose a random position and a random orientation. The construction of the chain proceeds then segment by segment. Let us consider the addition of one such segment. To be specific, let us assume that we have already grown $i-1$ segments, and that we are trying to add segment i. This is done as follows.

(1) Generate a fixed number (say k) of trial segments. The probability distribution of the orientations of the trial segments is proportional to the internal Boltzmann weight $P^{id}_{\hat{\mathbf{w}}_{i-1}\hat{\mathbf{w}}_j} = \exp[-\beta u^{id}_{\hat{\mathbf{w}}_{i-1}\hat{\mathbf{w}}_j}]$ associated with the internal bending. We denote the different trial segments by indices $1,2,\ldots,k$. Now the probability to generate a given subset $\{\hat{\mathbf{w}}\}_i$ of k trial segments with orientations $\hat{\mathbf{w}}_1$ through $\hat{\mathbf{w}}_k$ is equal to

$$P_{\{\hat{\mathbf{w}}\}_i} = \frac{1}{B^k}\prod_{j=1}^{k} d\hat{\mathbf{w}}_j P^{id}_{\hat{\mathbf{w}}_{i-1}\hat{\mathbf{w}}_j} . \tag{A1}$$

The normalization constant B is equal to $\int d\hat{\mathbf{w}}_j \exp[-\beta u^{id}_{\hat{\mathbf{w}}_{i-1}\hat{\mathbf{w}}_j}]$.

(2) For all k trial segments, we compute the "external" Boltzmann factor $\exp(-\beta u^{ext}_{\hat{\mathbf{w}}_j})$, where $u^{ext}_{\hat{\mathbf{w}}_j}$ is the potential energy of the jth trial segment of the polymer with conformation $\Gamma_{\mathbf{w}}$ due to interaction with all the other segments in the system.

(3) Select one of the trial segments, say $\hat{\mathbf{w}}_i$, with a probability

$$P^{ext}_{\hat{\mathbf{w}}_i} = \frac{\exp\left[-\beta u^{ext}_{\hat{\mathbf{w}}_i}\right]}{Z_{\{\hat{\mathbf{w}}\}_i}}, \tag{A2}$$

where we have defined

$$Z_{\{\hat{\mathbf{w}}\}_i} \equiv \sum_{j=1}^{k} \exp[-\beta u^{ext}_{\hat{\mathbf{w}}_j}].$$

The subscript $\{\hat{\mathbf{w}}\}_i$ means that $\hat{\mathbf{w}}_i$ is one of the segments of the subset, so $\hat{\mathbf{w}}_i \in \{\hat{\mathbf{w}}\}$.

(4) Add this segment as segment i to the chain and store the corresponding partial "Rosenbluth weight" [16]:

$$\omega_i = Z_{\{\hat{\mathbf{w}}\}_i}/k . \tag{A3}$$

In order to use this method to transfer a molecule from the reservoir to the system with N molecules in a GCMC simulation, we impose detailed balance on the Monte Carlo scheme. This implies that in equilibrium, the rate at which particles are removed from the system equals the reverse rate.

Let us first consider the grand canonical partition function in scaled coordinates of a combined system of N interacting particles in volume V and $M-N$ ideal polymers in a reservoir of volume V_{res}:

$$Q(M,V,V_{res},T) = \sum_{N=0}^{M} \frac{V^N V_{res}^{M-N}}{\Lambda^{3M} N!(M-N)!} \int ds^{M-N} \int d\Gamma^{M-N} \exp[-\beta V^{id}(\Gamma^{M-N})]$$

$$\times \int ds^N \int d\Gamma^N \exp\{-\beta[U^{id}(\Gamma^N) + U^{ext}(s^N)]\} , \tag{A4}$$

where $\Lambda = \sqrt{h^2/2\pi m k_B T}$, $U^{ext}(s^N)$ is the external potential of the N particles interacting with each other by a hard-core potential. $U^{id}(\Gamma^N)$ and $V^{id}(\Gamma^{M-N})$ are the internal potentials corresponding to the internal bending energy of the, respectively, N flexible chains in the system and $M-N$ flexible chains in the reservoir. The probability density $P(s^M;N)$ to find a system with $M-N$ particles at reduced coordinates s^{M-N} in a reservoir of volume V_{res} and N particles at reduced coordinates s^N in a system of volume V is

$$P(s^M;N) = \frac{V^N V_{res}^{M-N} \exp[-\beta V^{id}(\Gamma^{M-N})]}{N!(M-N)!\Lambda^{3M} Q(M,V,V_{res},T)}$$

$$\times \exp\{-\beta[U^{id}(\Gamma^N) + U^{ext}(s^N)]\} . \tag{A5}$$

The ratio of the statistical weights $P(s^M;N+1)$ and $P(s^M;N)$ is given by

$$\frac{P(s^M;N+1)}{P(s^M;N)} = \frac{V(M-N)\exp[-\beta(\sum_{i=1}^{L} u^{id}_{\hat{\mathbf{w}}_{i-1}\hat{\mathbf{w}}_i} + u^{\rm ext}_{\hat{\mathbf{w}}_i})]}{V_{\rm res}(N+1)\exp[-\beta\sum_{i=1}^{L} v^{id}_{\hat{\mathbf{w}}_{i-1}\hat{\mathbf{w}}_i}]} , \quad \text{(A6)}$$

where we have rewritten the difference in internal and external potential as follows:

$$U^{id}(\Gamma^{N+1}) + U^{\rm ext}(s^{N+1}) - U^{id}(\Gamma^N) - U^{\rm ext}(s^N) = \sum_{i=1}^{L} u^{id}_{\hat{\mathbf{w}}_{i-1}\hat{\mathbf{w}}_i} + u^{\rm ext}_{\hat{\mathbf{w}}_i} \quad \text{(A7)}$$

and

$$V^{id}(\Gamma^{M-N}) - V^{id}(\Gamma^{M-N-1}) = \sum_{i=1}^{L} v^{id}_{\hat{\mathbf{w}}_{i-1}\hat{\mathbf{w}}_i} . \quad \text{(A8)}$$

$v^{id}_{\hat{\mathbf{w}}_{i-1}\hat{\mathbf{w}}_i}$ denotes the internal potential associated with the internal bending of the chains in the reservoir.

The condition for detailed balance can now be expressed as follows:

$$P(s^M;N)G_{N\to N+1}P_{\rm acc}(N \mid N+1) = P(s^M;N+1)G_{N+1\to N}P_{\rm acc}(N+1 \mid N) , \quad \text{(A9)}$$

where $P(s^M;N)$ and $P(s^M;N+1)$ are, respectively, the statistical weights that the system has N particles and $N+1$ particles. $G_{N\to N+1}$ is the probability that, starting from the current configuration of N particles in the system, a configuration is generated with $N+1$ molecules in the system. $P_{\rm acc}(N \mid N+1)$ denotes the probability that this trial move is accepted. If we now impose the "superdetailed" balance condition, we have to consider the probability of generating a new chain in the system via one particular choice of trial directions $\{\hat{\mathbf{w}}_{\rm syst}\}_i$ and of choosing a set of trial directions in the reservoir $\{\hat{\mathbf{w}}_{\rm res}\}_i$ from all possible sets that contain the old configuration. The probability of transferring a chain of L segments from the reservoir to the system via the set $\{\hat{\mathbf{w}}_{\rm syst}\}_i$ and of choosing the set $\{\hat{\mathbf{w}}_{\rm res}\}_i$ will now be equal to the probability to generate the old set of trial directions $\{\hat{\mathbf{w}}_{\rm res}\}_i$ excluding the old orientation (denoted by $P_{\{\hat{\mathbf{w}}_{\rm res}\}_i}/\exp[-\beta v^{id}_{\hat{\mathbf{w}}_{i-1}\hat{\mathbf{w}}_i}]$) times the probability to generate a new set of trial directions in the system $\{\hat{\mathbf{w}}_{\rm syst}\}_i$ that contains the new orientation (i.e., $P_{\{\hat{\mathbf{w}}_{\rm syst}\}_i}$) times the probability to select this new orientation (i.e., $\exp[-\beta u^{\rm ext}_i]/Z_{\{\hat{\mathbf{w}}\}_i}$):

$$G_{N\to N+1} = \prod_{i=1}^{L} \frac{P_{\{\hat{\mathbf{w}}_{\rm syst}\}_i}P_{\{\hat{\mathbf{w}}_{\rm res}\}_i}}{\exp[-\beta v^{id}_{\hat{\mathbf{w}}_{i-1}\hat{\mathbf{w}}_i}]} \frac{\exp[-\beta u^{\rm ext}_i]}{Z_{\{\hat{\mathbf{w}}\}_i}} . \quad \text{(A10)}$$

The probability $G_{N+1\to N}$ is the probability of moving one chain from the system to the reservoir. The probability to exchange one particle with the reservoir is equal to the probability to generate the old set of trial directions in the system $\{\hat{\mathbf{w}}_{\rm syst}\}_i$ excluding the old orientation (i.e., $P_{\{\hat{\mathbf{w}}_{\rm syst}\}_i}/\exp[-\beta u^{id}_{\hat{\mathbf{w}}_{i-1}\hat{\mathbf{w}}_i}]$) times the probability to generate a new set of trial directions $\{\hat{\mathbf{w}}_{\rm res}\}_i$ that contains the new orientation (i.e., $P_{\{\hat{\mathbf{w}}_{\rm res}\}_i}$) times the probability to select this new orientation (i.e., $1/k$):

$$G_{N+1\to N} = \prod_{i=1}^{L} \frac{P_{\{\hat{\mathbf{w}}_{\rm res}\}_i}P_{\{\hat{\mathbf{w}}_{\rm syst}\}_i}}{\exp[-\beta u^{id}_{\hat{\mathbf{w}}_{i-1}\hat{\mathbf{w}}_i}]} \frac{1}{k} . \quad \text{(A11)}$$

The ratio of the probabilities $G_{N+1\to N}$ and $G_{N\to N+1}$ is now given by

$$\frac{G_{N+1\to N}}{G_{N\to N+1}} = \prod_{i=1}^{L} \frac{\exp[-\beta v^{id}_{\hat{\mathbf{w}}_{i-1}\hat{\mathbf{w}}_i}]}{\exp[-\beta(u^{id}_{\hat{\mathbf{w}}_{i-1}\hat{\mathbf{w}}_i} + u^{\rm ext}_{\hat{\mathbf{w}}_i})]} \frac{Z_{\{\hat{\mathbf{w}}\}_i}}{k} . \quad \text{(A12)}$$

Substitution of Eqs. (A6) and (A12) in Eq. (A9) yields

$$P_{\rm acc}(N \mid N+1) = \min\left(1, \frac{P(s^M;N+1)G_{N+1\to N}}{P(s^M;N)G_{N\to N+1}}\right) = \min\left(1, \frac{V(M-N)\mathcal{W}}{V_{res}(N+1)}\right) , \quad \text{(A13)}$$

where $\mathcal{W} = \prod_{i=1}^{L}\omega_i$. Let us now consider the limit that the reservoir is very much larger than the interacting system: $M\to\infty, V_{\rm res}\to\infty$ and $M/V_{\rm res}\to\rho$. For an ideal gas the fugacity z is equal to the particle density. Therefore, in the limit $M/N\to\infty$, Eq. (A13) becomes

$$P_{\rm acc}(N \mid N+1) = \min\left(1, \frac{Vz\mathcal{W}}{N+1}\right) . \quad \text{(A14)}$$

Similarly, we can derive the probability of accepting a trial move that removes a particle from the system to the reservoir:

$$P_{\rm acc}(N \mid N+1) = \min\left(1, \frac{N+1}{Vz\mathcal{W}}\right) . \quad \text{(A15)}$$

[1] P. J. Flory, Proc. R. Soc. London Ser. A **234**, 60 (1956).
[2] E. A. DiMarzio, J. Chem. Phys. **36**, 1563 (1962).
[3] P. J. Flory and G. Ronca, Mol. Cryst. Liq. Cryst. **54**, 289 (1979).
[4] G. Ronca, J. Polym. Sci. Pt. B **27**, 1795 (1989).
[5] J. F. Nagle, Proc. R. Soc. London Ser. A **337**, 569 (1974).
[6] A. Malakis, J. Phys. A **13**, 651 (1980).
[7] A. Baumgärtner, J. Chem. Phys. **84**, 1905 (1986).
[8] A. Kolinsky *et al.*, Macromolecules **19**, 2560 (1986).
[9] A. L. Rodriguez *et al.*, Macromolecules **23**, 4327 (1990).
[10] R. Dickman, Comput. Polym. Sci. **1**, 206 (1991).
[11] A. R. Khokhlov and A. N. Semenov, Physica A **108**, 546 (1981).
[12] A. R. Khokhlov and A. N. Semenov, Physica A **112**, 605

(1982).
[13] Z. Y. Chen, Phys. Rev. Lett. **71**, 93 (1993).
[14] M. P. Allen and D. J. Tildesley, *Computer Simulations of Liquids* (Clarendon, Oxford, 1987).
[15] D. Frenkel and R. Eppenga, Phys. Rev. A **31**, 3 (1985).
[16] D. Frenkel, G. C. A. M. Mooij, and B. Smit, J. Phys. Condens. Matter **4**, 3053 (1992).
[17] M. Dijkstra, D. Frenkel, and H. N. W. Lekkerkerker, Physica A **193**, 374 (1993).
[18] C. H. Bennett, J. Comput. Phys. **22**, 245 (1976).
[19] R. Eppenga and D. Frenkel, Mol. Phys. **52**, 1303 (1984).
[20] M. P. Allen and D. Frenkel, Phys. Rev. A **37**, 1813 (1988).
[21] M. P. Allen and D. Frenkel, Phys. Rev. A **42**, 3641 (1990).
[22] S. Ostlund and B. I. Halperin, Phys. Rev. B **23**, 335 (1981).
[23] J. V. Selinger and R. F. Bruinsma, Phys. Rev. A **43**, 2910 (1991).
[24] T. Odijk, Macromolecules **19**, 2313 (1986).
[25] H. Yamakawa and M. Fujii, J. Chem. Phys. **59**, 6641 (1973).